

# **Development of a Personal Sampler for Nanoparticles**

Final report on research carried out under  
National Institute for Occupational safety and Health (NIOSH)  
Research Grant: R01 OH009801

Prepared by

Principal Investigator: Yung Sung Cheng, Ph.D.  
505-348-9410, ycheng@LRRI.org

Research carried out at Lovelace Respiratory Research Institute  
2425 Ridgecrest Dr. SE, Albuquerque, NM 87108  
Starting Date: 9/1/2010– Ending Date: 8/31/2014

**November 2014**

## TABLE OF CONTENTS

LIST OF TERMS AND ABBREVIATIONS	3
ABSTRACT	4
SECTION 1	5
Highlights/Significant Findings	5
Translation Of Findings	5
Outcomes/Relevance/Impact	5
SECTION 2	6
Scientific Report	6
A. Background	6
B. Specific Aims	8
1. Specific Aim 1 .....	9
1.1 Personal Nanoparticle Sampler Development.....	9
1.2 Calibration of the Personal Sampler.....	11
2. Specific Aim 2 .....	16
2.1 Methodology .....	16
2.2 Aspiration Efficiency .....	19
3. Specific Aim 3 .....	23
3.1 Methodology .....	23
3.2 Results .....	24
4. Conclusions .....	28
Publications	28
Publications Generated from the Present NIOSH-funded Study	28
References	29

## LIST OF TERMS AND ABBREVIATIONS

ACGIH	American Council for Governmental Hygienists
ANSI	American National Standards Institute
CNT	carbon nanotubes
$d_{ae}$	aerodynamic diameter of aerosol
$d_{50}$	50 % cut-off diameter
EPA	Environmental Protection Agency
HEPA	high-efficiency particulate air MOUDI micro-orifice uniform deposit impactor
PENS	personal nanoparticle sampler
PSL	polystyrene latex
SEM	scanning electron microscope
SMPS	scanning mobility particle sizer
Stk	Stokes number
TEM	transmission electron microscope
U	Mean air velocity in the wind tunnel
VOAG	vibrating orifice monodisperse aerosol generator

## ABSTRACT

The development and commercialization of nanotechnology have been growing very rapidly over the past few decades. As more engineered nanomaterials are being incorporated into products or devices, concerns about potential environmental and occupational health implications also increase. In particular, workers in the nanotechnology-based industry deserve more attention as they may have the greatest risk to expose to engineered nanoparticles which leads to adverse health effects. Furthermore, many toxicological and epidemiological studies have shown that inhaled nanoparticles pose a higher adverse effect than that of large particles, because the number and surface area concentrations of engineered nanoparticles are much higher than those of large particles with the same mass. Therefore, the assessment of the potential occupational health risks due to the exposure to engineered nanoparticles is essential to ensure their safe manufacturing and handling in the workplaces.

Personal sampling is a better way to ensure accurate representation of the worker's exposure to ENMs than sampling at a fixed location. However, commercial samplers that sample particles in the nano-sized range such as the micro-orifice uniform deposit impactor (MOUDI), the low pressure impactor, or the electrical low pressure impactor, etc. are too heavy to be used as a personal sampler. The Marple Personal Cascade Impactor was developed as a personal cascade impactor with the 50% cutoff diameters of 21 to 0.4  $\mu\text{m}$  in its 0 to 8 stages and a backup filter, which does not cover the nano-sized range. There are no suitable personal samplers capable of assessing the exposure level of ultrafine particles or nanoparticles. The overall objective of this study is to develop a personal sampler capable of collecting the ultrafine particles (nanoparticles) in the occupational environment. This sampler consists of a cyclone for respirable particle classification, a micro-orifice impactor with a cutoff diameter of 100 nm for nanoparticle classification and a backup filter to collect nanoparticles.

Collection efficiencies of the cyclone and impactor stages were determined using monodisperse polystyrene latex and silver particles, respectively. Calibration of the cyclone and impactor stages showed 50% cut-off diameters of 4  $\mu\text{m}$  and 100 nm meeting the design requirements. Aspiration efficiencies of the sampler were measured in a wind tunnel at a flow rate of 2 L/min with wind speeds of 0.5, 1.0, and 1.5 m/s. The test samplers were mounted on a full size mannequin with three orientations toward the wind direction (0°, 90°, and 180°). Monodisperse oleic acid aerosols tagged with sodium fluorescein in the size range of 2 to 10  $\mu\text{m}$  were used in the test. For particles smaller than 2  $\mu\text{m}$ , the fluorescent polystyrene latex particles were generated by nebulizers. Results showed that the orientation-averaged aspiration efficiency for both samplers were close to the inhalable fraction curve. Our evaluation showed that the current design of the personal sampler met the designed criteria for collecting nanoparticles  $\leq 100$  nm in occupational environments.

Comparison of  $\text{TiO}_2$  and carbon nanotube nanoparticles collection in the personal sampler with MOUDI impactor show good agreement indicating that the personal sampler is useful for collecting nanoparticles.

## **SECTION 1**

### **Highlights/Significant Findings**

1. Prototype of personal nanoparticle sampler with a cyclone and micro-impactor stages were designed, developed and fabricated. Modifications have been made on the prototype that has met the design criteria.
2. Pressure drop of the sampler is within the operational range of a personal sampling pump.
3. Laboratory calibration of cyclone and micro-impactor stages showed the collection efficiency with 50% cutoff diameter of 4  $\mu\text{m}$  and 100 nm meeting the design specification.
4. The aspiration efficiencies obtained from the newly developed personal bioaerosol samplers were measured in a large wind tunnel on the lapel of a manikin. The orientation-averaged aspiration efficiency agreed well with the ACGIH inhalable convention.
5. Comparison of  $\text{TiO}_2$  and carbon nanotube nanoparticles collection in the personal sampler with MOUDI impactor show good agreement indicating that the personal sampler is useful for collecting nanoparticles.

### **Translation Of Findings**

In this study we designed a new personal sampler and conducted performance evaluations for the newly developed nanoparticle personal sampler in various aspects. The results acquired provide considerable insight into the characteristics on physical sampling and collection efficiency, which substantially assist the goal of achieving collection of nanoparticles for mass concentration determination and providing samples for further analyses.

### **Outcomes/Relevance/Impact**

A personal nanoparticle bioaerosol sampler was designed, fabricated and tested. The new nanoparticle personal sampler can obtain samples of nanoparticles smaller than 100 nm for various analyses. The aspiration efficiency of the sampler was found to match the ACGIH inhalable convention well, which indicates that the personal sampler is able to accurately collect bioaerosol samples in the inhalable particulate matter fraction around the wearer. The collection efficiencies of the cyclone and impactor stage indicate that it could collection fractions of particles smaller than 100 nm and between 100 nm and 4  $\mu\text{m}$ . This result will greatly benefit to those workers in nanomaterial work environments, for actual assessing the mass concentration of personal exposure as well as providing samples for further analyses.

## SECTION 2

### Scientific Report

#### A. Background

Nanoparticles (or ultrafine particles) are those materials with at least one dimension  $\leq 100$  nm and have very large surface areas with increased chemical and biological reactivity compared to the bulk material. Nanoparticles can be released in the ambient environment from high-temperature sources, including industrial processes and mobile combustions (Biswas and Wu, 2005). Recently, the advances of nanotechnology have produced a diverse range of nanomaterials such as metal oxides, fullerenes; nanotubes, nanowires, and quantum dots (Hoet et al., 2004). These materials are called “engineered nanoparticles.” The application of engineered nanomaterials has grown rapidly into all sectors of our society. The explosive development of nanomaterials has raised concerns about potential exposure and associated health effects (Kreyling et al., 2004; Maynard et al., 2004; Hoet et al., 2004; Biswas and Wu, 2005).

Recently several studies of exposure assessment in nanomaterial production facilities showed that the mass concentration of nanoparticles were generally higher than those of ambient environment. The chemical composition and size distribution of engineered nanoparticles were more defined and specific for each production facilities (Maynard et al., 2004; Demou et al., 2008; Yaganeh et al., 2008).

A potential important human exposure route for nanoparticle includes exposure followed by exposure via inhalation, skin and the gastrointestinal tract (Oberdorster et al., 2005). Inhaled nanoparticles deposit with high efficiency in all regions of respiratory tract by the diffusion process (Cohen and Asgharian 1990; Cheng et al., 1996; Smith et al., 2001; Asgharian and Price, 2007). Because of greater surface areas, inhaled nanoparticles showed greater inflammatory responses on a given mass than do larger particles with the same chemical composition (Oberdorster et al., 2005). There are many epidemiological and controlled clinical studies of adverse health effects on exposure to ambient ultrafine particles (Oberdorster et al., 2005).

Several instruments are available for monitoring nanoparticle concentrations. A nanoparticle surface area monitor uses diffusion charging of particles followed by electrometer detection to determine the particle concentration (Fissan et al., 2007). Another frequently used direct-reading instrument is the scanning mobility particle spectrometer (SMPS) for measuring concentration and size distribution of submicron aerosols including nano-sized particles (Wang and Flagan 1990). Both instruments do not collect particles and are not personal samplers for mass concentration determination.

To take samples and determine the mass concentration of nanoparticles, the sampling device needs to separate particles  $\leq 100$  nm from the aerosol stream and collect this fraction. Micro-orifice cascade impactors including the MOUDI and Nano-MOUDI are available to aerodynamically separate particles down to nanoparticle size fractions and collect these fractions. But these samplers are too bulky to be used for personal sampling. The Marple Personal Cascade Impactor was developed as a personal cascade impactor with the 50% cutoff diameter of 21 to 0.4  $\mu\text{m}$  in its 0 to 8 stages and an after filter, which does not cover the nano-sized range (Rubow et al., 1987).

Several studies have been devoted to the development of a personal nanoparticle sampler. For example, a thermal precipitator was designed as a personal sampler to deposit nanoparticles uniformly on a colder plate by a uniform temperature gradient (Azong-Wara et al., 2009; Thayer et al., 2011). The morphology, crystallography, and chemical composition of the deposited particles could be further analyzed by using the scanning electron microscope (SEM) or transmission electron microscope (TEM). The quantitative number concentrations can be estimated from the particles deposited on the TEM grids with the use of a model established by Lorenzo et al. (2007). Miller et al. (2010) developed a handheld electrostatic precipitator to deposit nanoparticles on the substrate with collection efficiencies from 76 to 94% for nanoparticles ranging from 30 to 400 nm in diameter. However, these samplers

were designed for physical and chemical characterization of nanomaterial but did not collect enough material for mass concentration determination.

The current monitoring devices for nanoparticles are either direct-reading devices that do not provide samples for analysis or samplers that collect nanomaterials for physical and chemical characterization. There is a need to develop a light-weight small-volume personal sampling device that can classify the nanoparticle fraction ( $\leq 100$  nm) from the aerosol stream and collect this fraction for various analyses including mass concentration determination.

The overall objective of this study is to develop a personal sampler capable of collecting the ultrafine particles (nanoparticles) in the occupational environment. This sampler consists of a cyclone for respirable particle classification, a micro impactor stage to achieve nanoparticle classification, and a backup filter to collect nanoparticles.

## **Specific Aims**

**Specific Aim 1:** To design and fabricate a personal sampler to collect nanoparticles  $\leq 100$  nm in diameter. This sampler is capable of separating and collecting nanoparticles in a backup filter to assess the workplace exposure. We will also measure the flow rate and pressure drop of the sampler, which are important parameters for personal sampling and in the selection of a sampling pump.

**Specific Aim 2:** To characterize the personal sampler in terms of aspiration efficiency and particle losses in the prototype sampler. This study will enable us to assess the efficacy of the sampler indoors, similar to many workplace conditions, and may offer insight into necessary design modifications for optimal performance.

**Specific Aim 3:** To evaluate the performance of the sampler in collecting the nanoparticle fraction of nanomaterials including  $\text{TiO}_2$ , and carbon nanotubes in the laboratory. The collection of the nanoparticle fraction will be compared with standard area samplers for nanoparticles such as a micro-orifice uniform deposition impactor (MOUDI).



**1. Specific Aim 1: To design and fabricate a personal sampler to collect nanoparticles  $\leq 100$  nm in diameter.**

**1.1 Personal Nanoparticle Sampler Development**

As shown in Figure 1, the present sampler consists of three main parts. The first part is a respirable cyclone, which is used to classify particles larger than  $4 \mu\text{m}$  in aerodynamic diameter ( $d_{ae}$ ). The second part is a micro-orifice impactor with the cut-point of  $100 \text{ nm}$ . Particles ranging from  $100 \text{ nm}$  to  $4 \mu\text{m}$  will impact on the impaction plate while nanoparticles are collected by the final part, which is a filter cassette containing a  $37 \text{ mm}$  Teflon filter (Teflo R2PL037, Pall Corp., New York, USA). The size and weight of the personal sampler are  $107 \text{ mm}$  (length)  $\times$   $44 \text{ mm}$  (width) and  $240 \text{ g}$ , respectively. The sampling flow rate is kept at  $2 \text{ L/min}$  to ensure the pressure drop of the sampler,  $14.1 \text{ kpa}$  (respirable cyclone:  $0.1 \text{ kpa}$ , micro-orifice impactor:  $13 \text{ kpa}$ , Teflon filter:  $1 \text{ kpa}$ ), is within the maximum allowable pressure drop of  $21 \text{ kpa}$  for the personal sampling pump (AirChek XR5000, SKC Inc., Eighty Four, PA) used in the study. The XR-5000 pump is able to drive the sampler for more than 12 hours, which is long enough for the 8 hours duration of a typical work shift.

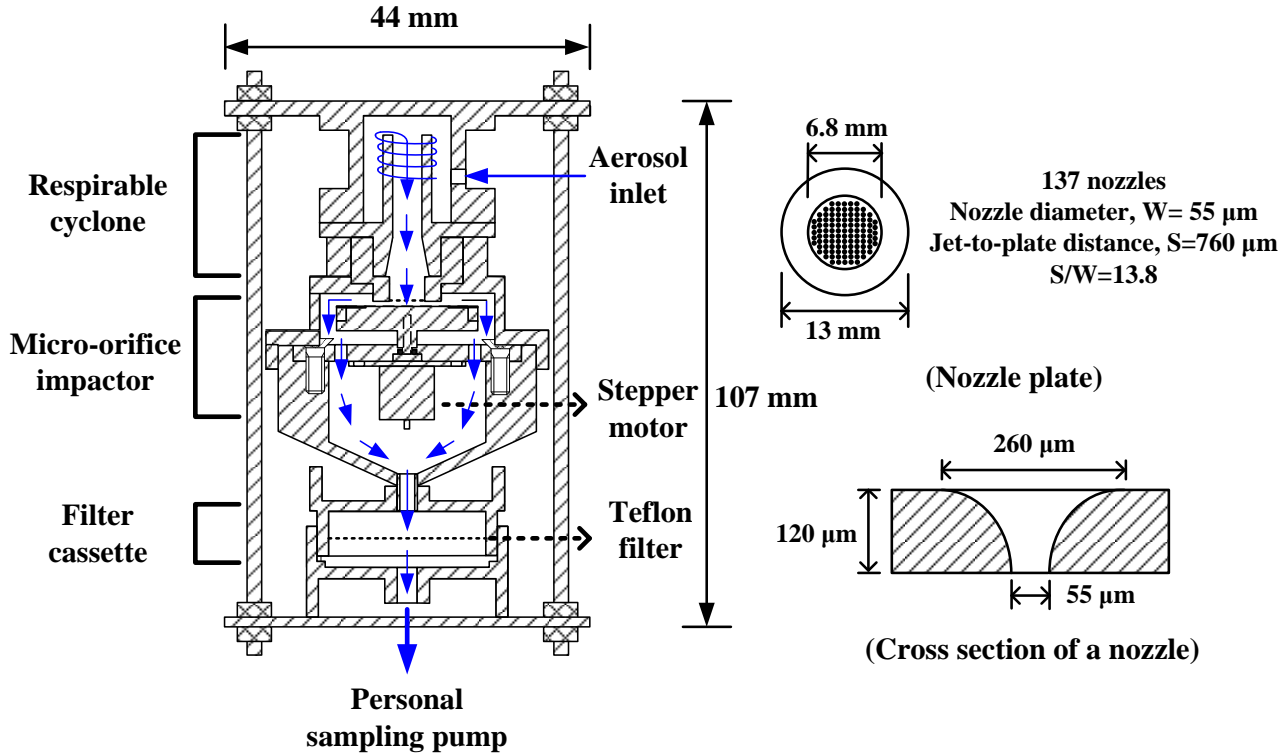


Figure 1. Schematic of a two-stage personal nanoparticle sampler.

The design of the present respirable cyclone is different from that of the conventional tangential flow cyclone (Tsai et al., 1999). Instead of upward direction, the air flow from the vortex finder of the cyclone exits downward directly into the micro-orifice impactor to facilitate the compact assembly of the sampler.

The respirable cyclone was designed based on the dimensionless parameter,  $\sqrt{Stk_{50}}$ , the square root of the cut-off Stokes number, which is defined as (Blachman and Lippmann, 1974):

$$\sqrt{Stk_{50}} = \sqrt{\frac{C_c \rho_p d_{ae50}^2 U_i}{9\mu D}} \quad (1)$$

Where  $C_c$  is the slip correction factor,  $\rho_p$  is the particle density,  $d_{ae50}$  is the cut-off aerodynamic diameter,  $U$  is the gas velocity at the inlet,  $\mu$  is the air dynamic viscosity, and  $D$  is the inner diameter of the cyclone. The design of the respirable cyclone was similar to the 18-mm respirable cyclone developed by Tsai et al. (1999), except that the flow direction from the vortex finder was different. For  $d_{ae50}=4 \mu\text{m}$ , the side length of the tangential square inlet opening was calculated to be 2.4 mm at the sampling flow rate of 2 L/min based on Equation (1). Later, the laboratory calibration showed that the  $d_{ae50}$  was 4.7  $\mu\text{m}$ . The inlet dimension was then reduced to 2.1 mm to achieve the  $d_{ae50}$  close to 4.0  $\mu\text{m}$ .

The  $d_{ae50}$  of the micro-orifice impactor was designed to be 100 nm. The design was also based on Equation (1) in which  $D$  and  $U$  were replaced by the nozzle diameter and air speed at the nozzle,

respectively. Referring to  $\sqrt{Stk_{50}}$  of the 9<sup>th</sup> stage of the MOUDI (Marple et al., 1991), which is 0.62, the micro-orifice plate was designed to have 137 nozzles, each of which is 55  $\mu\text{m}$  in the inner diameter. The nozzle plate with the effective diameter of 6.8 mm for the nozzles was manufactured by a semiconductor process to have a smooth nozzle shape, as shown in Figure 1. To achieve a uniform particle deposition and avoid solid particle bounce, a stepper motor (SPC-15RF, Epoch Electronics Corp., Japan) powered by eight AA Ni-MH (Nickel-Metal Hydride) rechargeable batteries was used to rotate the impaction plate at 1 rpm while the nozzle plate was fixed.

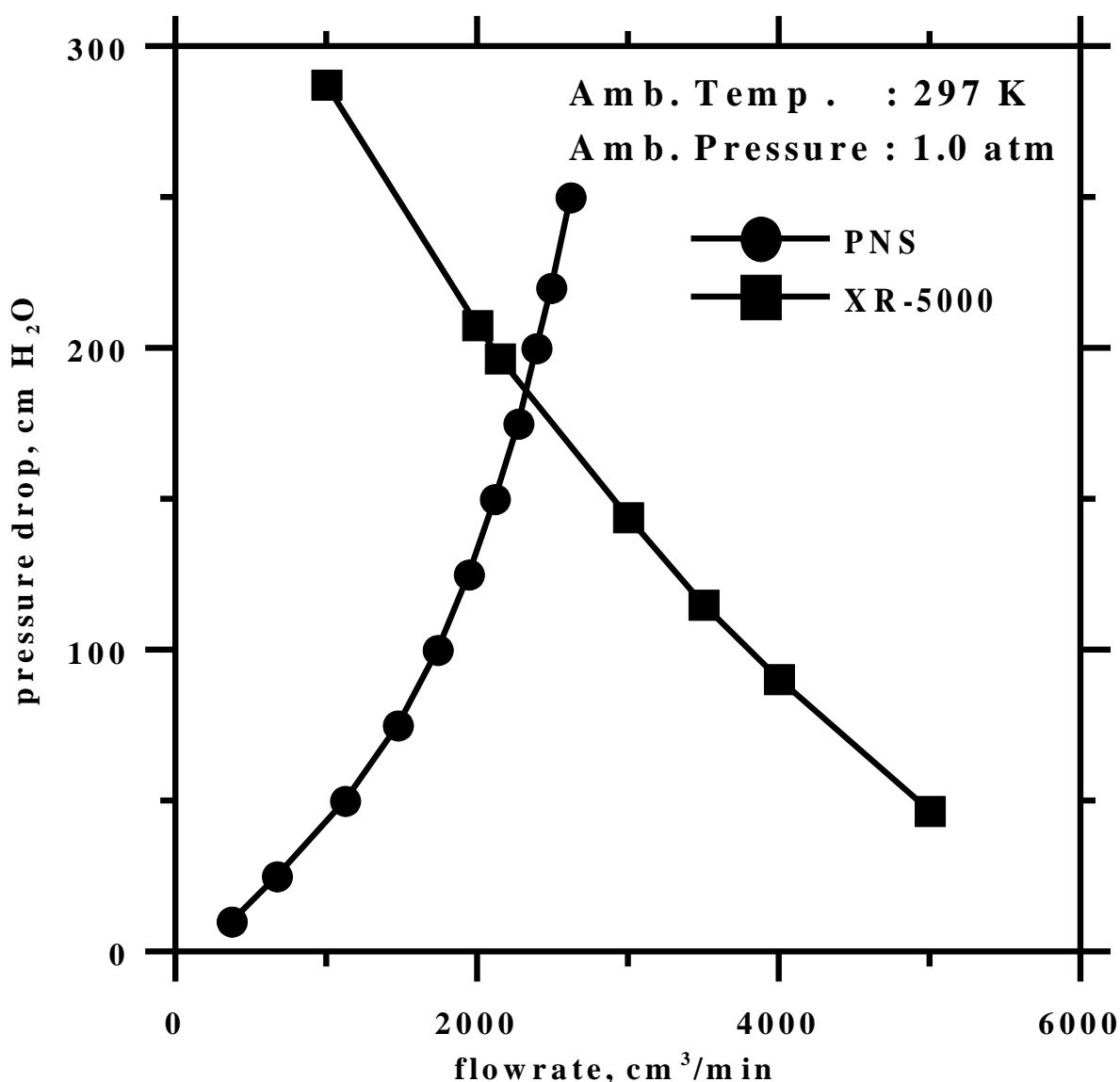


Figure 2. Pressure drops of the personal nanoparticle sampler and a personal sampling pump (XR-5000).

## 1.2 Calibration of the Personal Sampler

### 1.2.1 Pressure Drop

Figure 2 shows the relationship of the pressure drop versus flow rate of the personal nanoparticle sampler (PENS) and the performance curve of the personal sampling pump (AirChek XR5000, SKC Inc., Eighty Four, PA), when the Teflon filter was not installed in the PENS during the measurement. At the sampling flow rate of 2 L/min, the pressure drop through the PENS is about 133 cm H<sub>2</sub>O (or 13 kpa), which is much lower than the maximum allowable pressure drop of the personal pump, 210 cm H<sub>2</sub>O (or 21 kpa). When a Teflon filter was installed in the PENS, the pressure drop was increased slightly to 145 cm H<sub>2</sub>O (14 kpa) at 2 L/min, indicating that there is still an enough margin for a possible pressure drop increase due to nanoparticles collected on the filter. However, further increase in the sampling flow rate may exceed the capacity of the pump.

### 1.2.2 Cyclone Calibration

Figure 3 shows the experimental setup for the calibration of the cyclone stage of the personal sampler. Monodisperse sodium-fluorescein-tagged oleic acid particles with a particle size range of 2.5-9  $\mu\text{m}$  were generated by a vibrating orifice monodisperse aerosol generator (VOAG, Model 3050, TSI Inc., St. Paul MN). An aerodynamic particle sizer (TSI Inc.) was used to monitor and adjust the aerosol size distribution. Only aerosols with a geometric standard deviation (GSD)  $<1.2$  were considered as monodisperse. For 2  $\mu\text{m}$  particles generated by the VOAG, the GSD was  $>1.2$ , which is not considered monodisperse. The polystyrene latex (PSL) fluorescent aerosols (Duke Scientific, Palo Alto, CA) were generated by a medical nebulizer (Hospitak, Lindenhurst, NY) only for this particle size. Monodisperse aerosols were generated and neutralized by a Kr-85 source before entering the chamber. When the nebulizer was used as an aerosol generator, the vibrating orifice monodisperse aerosol generator was used as an air dilutor to provide enough air to the chamber.

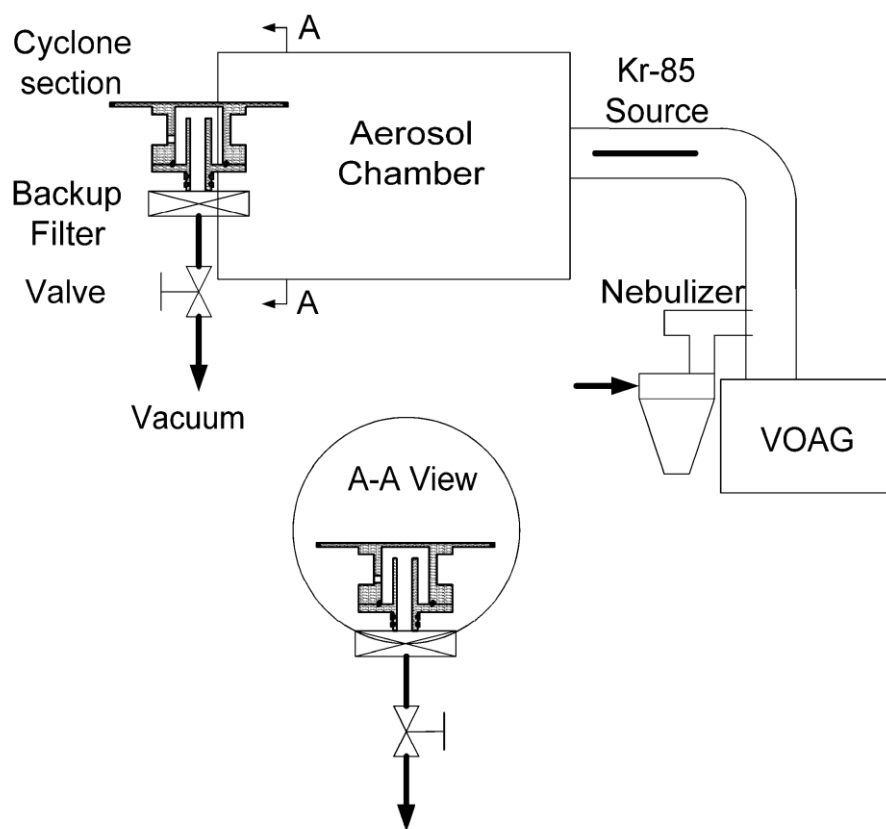


Figure 3. Experimental setup for the calibration of the cyclone stage of the personal nanoparticle sampler.

After each test, particles deposited in the sampler and backup filter were rinsed out by using a solution consisting of 50% isopropyl and 50% distilled water for oleic acid particles and with 100% ethyl acetate for PSL particles. The filters were also placed in the solutions for 24 hours. The relative concentrations of fluorescent tracers in the solutions were measured with a fluorometer (Model 450, Sequoia-Turner Corp. Mountain View, CA). One drop (35–40  $\mu\text{L}$ ) of 1 N NaOH was applied into each glass tube, which contains around 6 mL of sample to stabilize the fluorescence. The relative concentration of the fluorescent tracer in the solution was calculated by taking account of the sampling flow rate, sampling time, and dilution factor. The deposition efficiency of the samplers was obtained by dividing the relative concentration of the fluorescent tracer in the device by relative concentration of the fluorescent tracer in the device and filter. Each data point was an average value of triplicate tests.

The cyclone was initially tested at National Chiao Tung University, Taiwan, with different method and particles. Oleic acid liquid droplets were generated using an Ultra sonic atomizer (Model 06-05108, Sono-Tek, NY). The concentrations upstream and downstream of the cyclone were measured by an Aerodynamic Particle Sizer (APS Model 3321, TSI Inc., St Paul, MN). The concentration ratio was used to calculate the collection efficiency as function of particle size.

Figure 4 shows the collection efficiency curves from the National Chiao Tung University and Lovelace Respiratory research institute (LRRRI), showing the data were in agreement. A fitted curve was obtained by the nonlinear regression routine of SigmaPlot (SPSS Inc., Chicago, IL) showing the collection efficiency  $E$  as a function of the aerodynamic diameter. Based on the calibration curve, 50% cutpoint diameter of the test is  $3.95 \pm 0.3 \mu\text{m}$ , while the result from the National Chiao Tung University is  $4.05 \pm 0.16 \mu\text{m}$ .

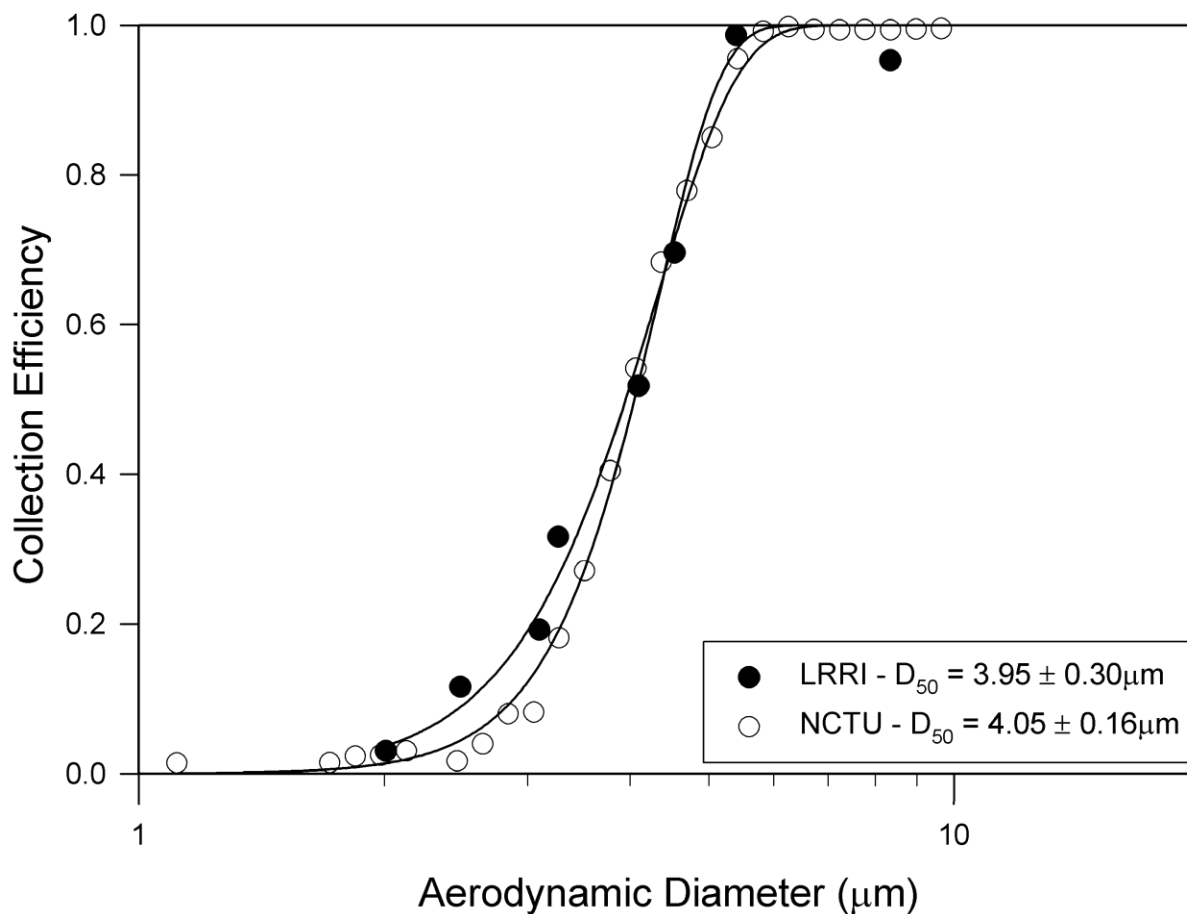


Figure 4. Collection efficiency of the cyclone stage as a function of the aerodynamic diameter.

### 1.2.3 Micro-orifice impactor Calibration

Figure 5 shows the experimental setup for collection efficiency test of the micro-orifice impactor. Silver aerosols were generated using the condensation aerosol generation method (Cheng et al., 1995). Silver wool was placed in a quartz boat inside a quartz tube of tube furnace. The furnace was operated at 700-900 °C. Filtered dry air at a flow rate of 1 L/min carried the vaporized materials into a glass condensation chamber, where the vapor was condensed into nano size particles. Particles were then introduced into an electrostatic classifier to classify to single charged monodisperse aerosols. A scanning mobility particle sizer (SMPS, TSI Inc.) was used to verify the relations between particle size and voltage of the classifier. The monodisperse particles were then delivered into a mixing chamber where dilute air was provided. The micro-orifice impactor sampled aerosols from the mixing chamber. Aerosol concentrations at the inlet and outlet ports of the micro-orifice impactor were determined by a condensation particle counter (CPC, TSI Inc.). The deposition efficiency of the impactor can be calculated by the ratio of aerosol concentration in the outlet and inlet of the impactor. The particle size range was 50 to 300 nm.

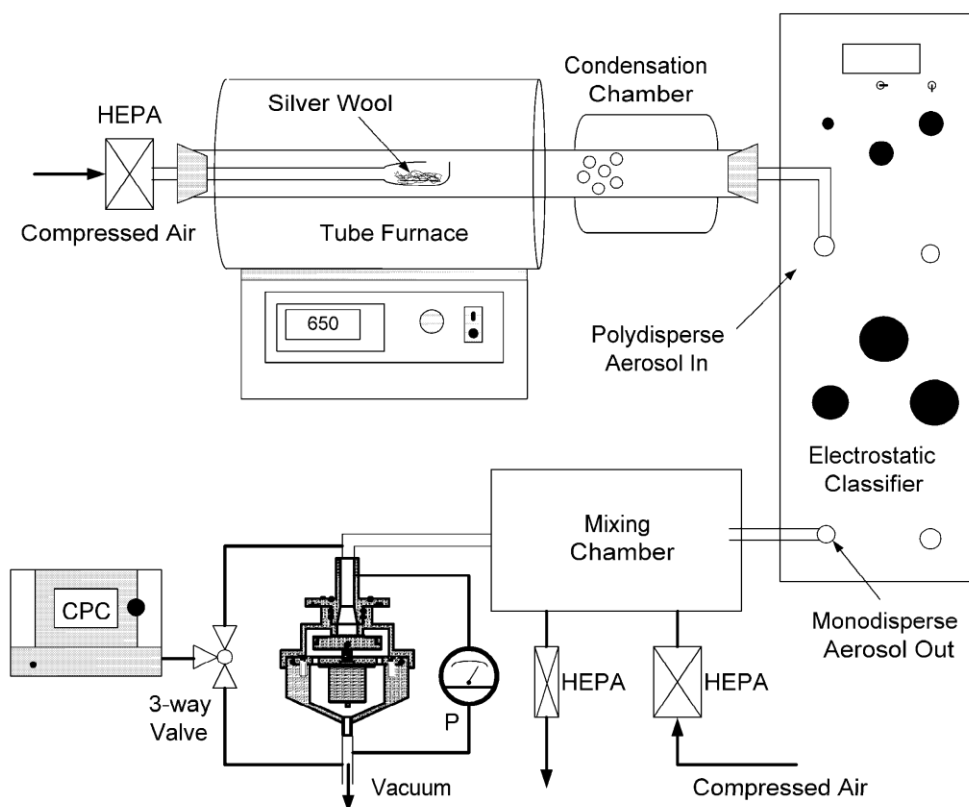


Figure 5. Experimental setup for the calibration of the impactor stage of the personal nanoparticle sampler.

Figure 6 shows collection efficiency curve of the micro-orifice impactor. With the data fitting of the collection efficiency curve, the 50% cutpoint diameter of the test is  $94.7 \pm 29.0$  nm, while the result from the National Chiao Tung University using oleic acid particles is  $101.4 \pm 0.1$  nm

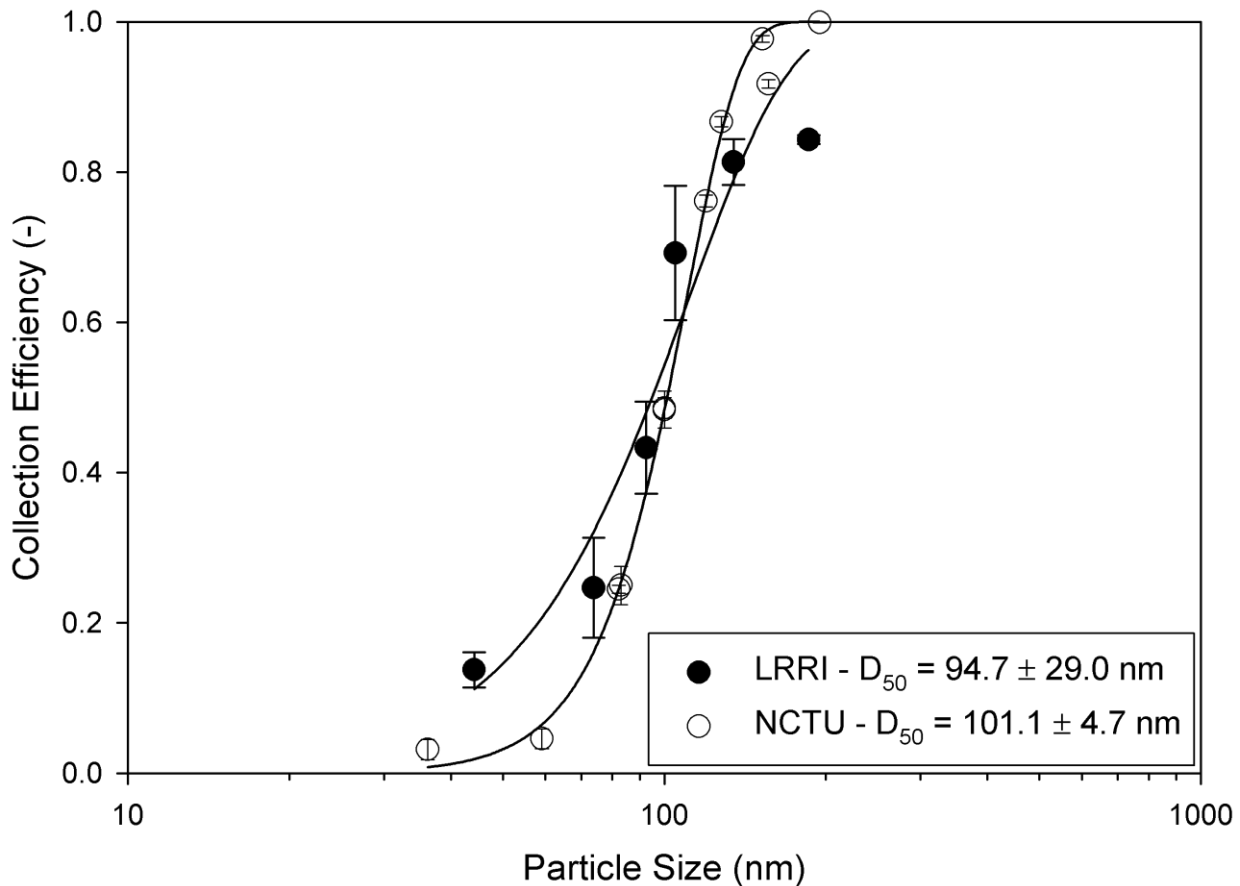


Figure 6. Calibration curves of the impactor stage of the personal nanoparticle sampler.

## 2. Specific Aim 2: To characterize the personal sampler in terms of aspiration efficiency and particle losses in the prototype sampler.

### 2.1 Methodology

#### 2.1.1 Wind Tunnel

All measurements were made in a wind tunnel inside of a 4.3 x 3.7 x 3.6 m test room. The wind tunnel consists of an 11-m-long circular duct with a diameter of 1.83 m; a stationary air blender (Blender Products, Inc. Denver, CO), which creates mixing; and a flow straightener, test chamber, and blower (Figure 7). Incoming air filtered by a high-efficiency particulate air (HEPA) filter is drawn from the specially designed test room into the open-loop flow and exhausted to the same room. The blower used for the wind tunnel (IAP, Inc., Phillips, WI) has a capacity of 1100 m<sup>3</sup>/m at 1.25 kpa static pressure. The wind velocity in the wind tunnel can be adjusted from 0.5 to 8.0 m/s by changing the speed of the blower motor. The wind tunnel was calibrated according to U.S. Environmental Protection Agency (EPA) and American National Standards Institute (ANSI) standards. The coefficient of variation (COV) of the wind speeds measured in the middle two-thirds of the test section was found to be less than 5% for all of those wind speeds within the range specified by the EPA and ANSI N13.1 (i.e., 10% over the middle two-thirds of the cross-sectional area). The uniformity of the aerosol concentration in the test



section was measured using a 10- $\mu\text{m}$  test aerosol. The COVs of the aerosol concentration were 7.5, 9.1, and 7.5% for wind speeds of 0.56, 2.2, and 6.6 m/s respectively. The calibration details were described previously in Cheng et al. (2004).

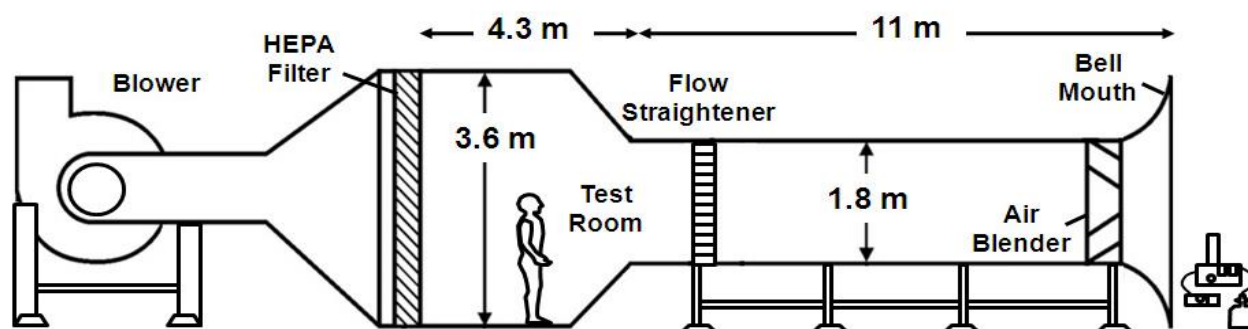


Figure 7. Schematic of the LRR large wind tunnel facility.

### 2.1.2 Test Aerosols

The vibrating orifice monodisperse aerosol generator (VOAG) was used to generate monodisperse, sodium-fluorescein-tagged oleic acid aerosols with the size of 3 to 10  $\mu\text{m}$ . For particles smaller than 3  $\mu\text{m}$ , four Hospitak nebulizers were used to generate PSL particles. The VOAG or nebulizers were placed immediately outside of the wind tunnel entrance. The air with generated particles traveled through the length of the wind tunnel and the flow straightener to dampen the turbulence before entering the test chamber. Particles in the range of 0.7 to 10  $\mu\text{m}$  were used in the study. The test aerosol size was determined by an aerodynamic particle sizer (APS Model 3310A, TSI Inc.).

### 2.1.3 Experimental Set-up and Procedures

A NIOSH-designed personal sampler used for collecting bioaerosol consists of two cyclones and a backup filter (Lindsley et al., 2006). The 50% cutoff aerodynamic diameters for the two cyclones are 2.6  $\mu\text{m}$  and 1.6  $\mu\text{m}$  at 2.1 L/min sampling flow rate. The NIOSH sampler was tested for aspiration efficiency in this study in comparison with the PENS sampler.

Three PENS and three NIOSH samplers were mounted on a full-size mannequin (170 cm) at a height of 150 cm. One of each type was mounted at the chest of the mannequin, one on the back, and one at a side of mannequin (Figures 8 and 9). Cellulose filters (Type 41, Whatman, Inc., Florham Park, NJ) were used to collect particles passing through the PENS and NIOSH samplers. The samplers were operated at a flow rate of 2.0 L/min with wind speeds of 0.5, 1.0, and 1.5 m/s.

Two isokinetic samplers were operated at a sampling flow rate of 68  $\text{m}^3/\text{h}$  controlled by a Venturi orifice downstream of the filter (Model G10557PM10, Thermo Andersen, Smyrna, GA). The test aerosol was sampled with a 20 cm x 25.4 cm glass-fiber filter (EPM 2000, Whatman Inc., Clifton, NJ).

After each test, particles deposited in the samplers were rinsed out by using a solution consisting of 50% isopropyl and 50% distilled water for oleic acid particles and with 100% ethyl acetate for PSL particles. All filters were also placed in the solutions for 24 hours. The relative concentrations of fluorescent tracers in the solutions were measured with a fluorometer (Model 450, Sequoia-Turner Corp. Mountain View, CA). One drop (35–40  $\mu\text{L}$ ) of 1 N NaOH was applied into each glass tube, which contains around 6 mL of sample to stabilize the fluorescence. The relative concentration of the fluorescent tracer in the solution was calculated by taking account of the sampling flow rate, sampling time, and dilution factor. By dividing the relative concentration of the sampler device and backup filter solutions by the relative concentration of the reference filter solution and wall wash solution, the aspiration efficiency, was calculated.



Figure 8. Photo of the test room of the LRR1 wind tunnel showing the full-size mannequin with the tested samplers and the two reference filter samplers.

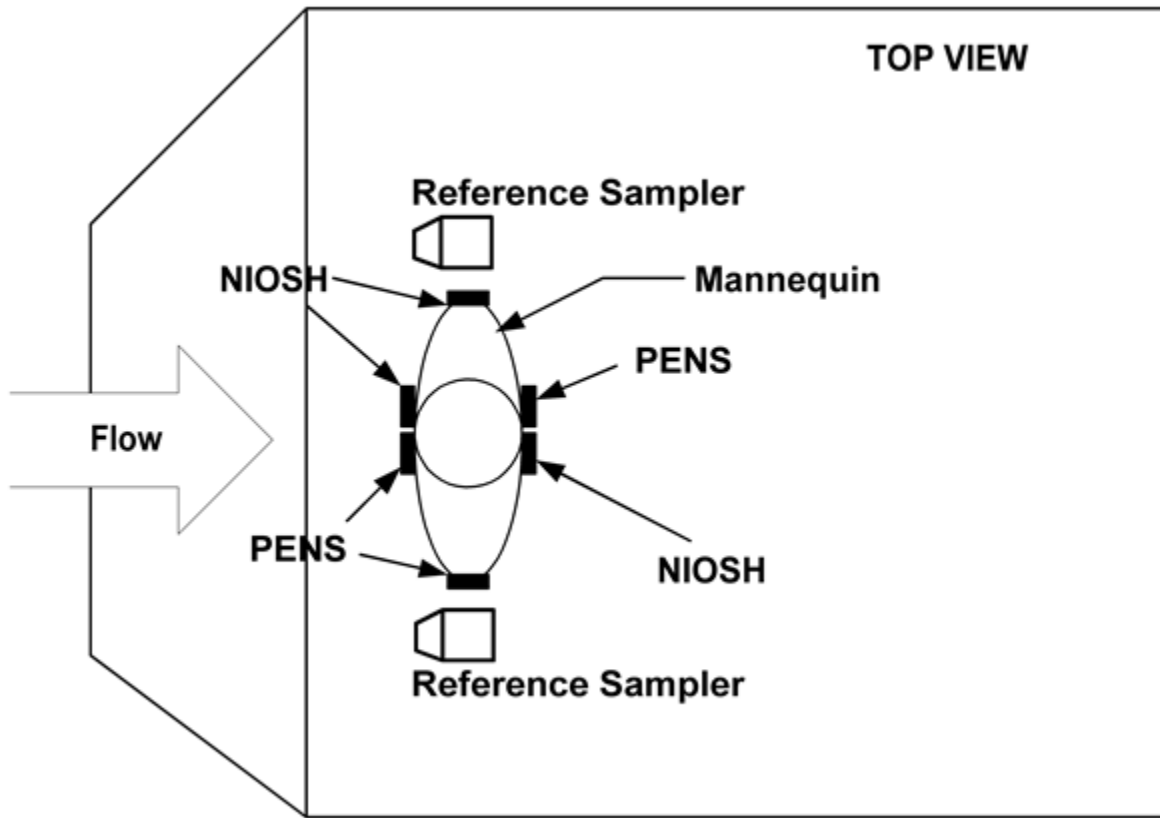


Figure 9. Top view of the test room of the LRRI wind tunnel showing the full-size mannequin with the tested samplers and the two reference filter samplers.

## 2.2 Aspiration Efficiency

Figure 10 shows the orientation-averaged aspiration efficiency for both PENS and NIOSH samplers compared to the inhalable convention curve at the wind speeds of 0.5 (A), 1.0 (B), and 1.5 (C) m/s.

The ACGIH inhalable fraction (IF) equation for occupational sampling criteria can be expressed in the following equation (Phalen et al., 1986):

$$IF = [1 - F(x)], \quad (2)$$

Where  $F(x) = \int_{-\infty}^x \frac{dy}{\sqrt{2\pi}} \exp(-y^2/2)$  is a function of aerodynamic diameter  $d_{ae}$

$$y = \frac{\ln(d_{ae} / d_{ae50})}{\ln(\sigma_g)}; d_{ae50} \text{ (at 50 \% penetration) } = 10 \mu\text{m}; \text{ and } \sigma_g = 1.5. \quad (3)$$

The root-mean-square deviation (RMSD) was used for the results in comparing to the inhalable fraction equation:

$$\text{RMSD} = \sqrt{\frac{\sum_{i=1}^n (Y_i - IF_i)^2}{n}} \quad (4)$$

Where the  $Y_i$  is the observed value,  $IF_i$  is the modelled value, and  $n$  is the number of data points. The value of RMSD should be between 0 and 1. All data points are on the equation curve if the RMSD is zero. The smaller the RMSD value, the closer the data point is to the curve.

Table 1. The RMSDs for all wind speeds and wind directions

Wind Speed (m/s)	0.5		1.0		1.5		0.54
Sampler	PENS	NIOSH	PENS	NIOSH	PENS	NIOSH	IOM <sup>A</sup>
0°	0.18	0.38	0.57	0.39	0.44	0.43	0.30
90°	0.55	0.34	0.32	0.48	0.33	0.28	0.22
180°	0.68	0.46	0.40	0.41	0.44	0.32	0.25
Avg <sup>B</sup>	0.17	0.21	0.34	0.27	0.31	0.29	0.26

<sup>A</sup> the flow rate of the IOM is 2 L/min

<sup>B</sup> orientation-averaged

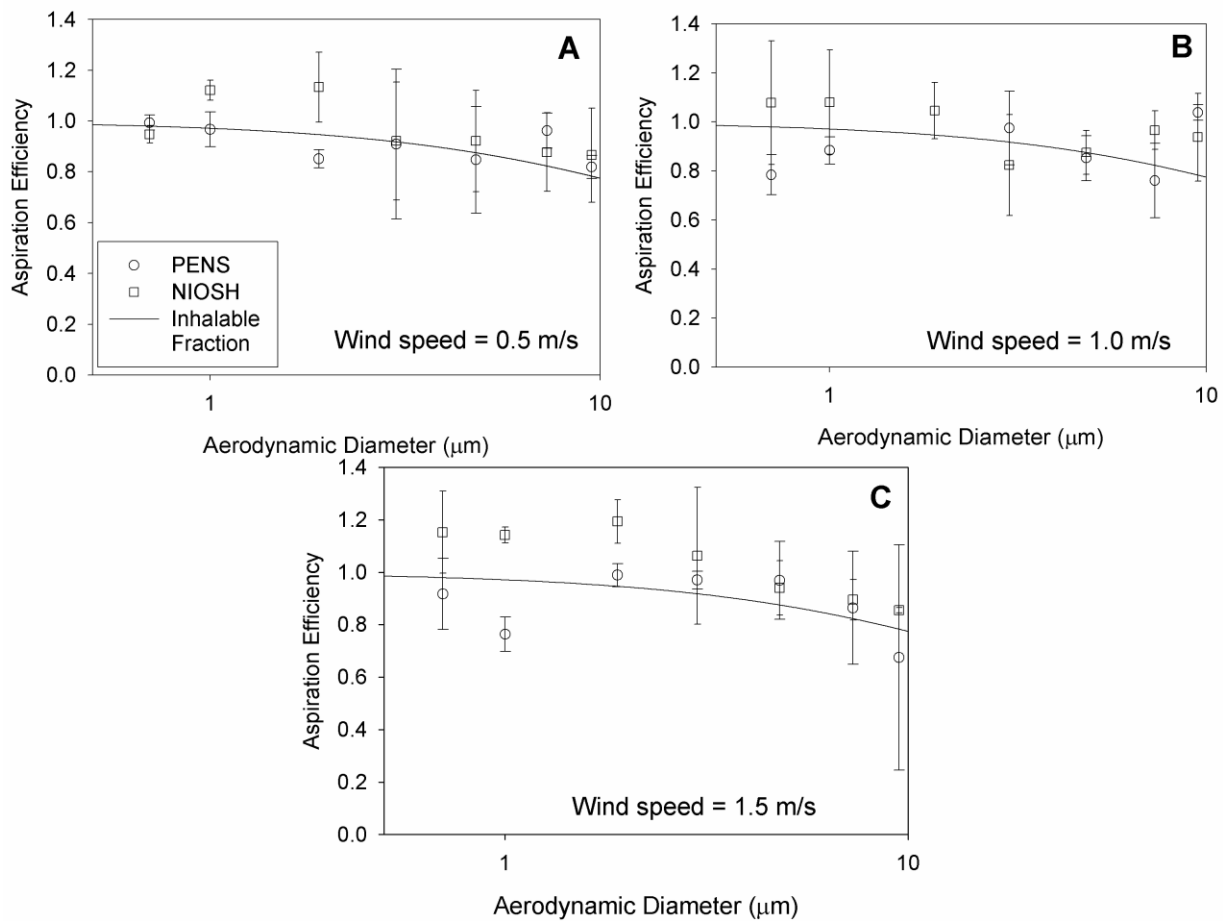


Figure 10. Orientation-averaged aspiration efficiencies for PENS and NIOSH samplers with a comparison of inhalable fraction curve at the wind speeds of 0.5 (A), 1.0 (B), and 1.5 (C) m/s.

Figure 10 shows the orientation-averaged aspiration efficiency for both PENS and NIOSH samplers compared to the ACGIH inhalable fraction curve at the wind speeds of 0.5 (A), 1.0 (B), and 1.5 (C) m/s. The results of three wind directions (0°, 90°, and 180°) were shown in Figure 11 at different wind speeds. For small particles, it is possible that particle concentration collected with the sampler is higher than that collected on the reference filters. This will result the aspiration efficiency larger than 1. Table 1 listed the RMSD for different wind speed and orientations. The average RMSDs for different wind speeds were also listed. For a comparison, the RMSDs from previous study for IOM samplers (Zhou and Cheng 2010) were included. For the PENS sampler, most of the orientation-averaged aspiration efficiency data points were around the inhalable curve at a wind speed of 0.5 m/s. However, the aspiration efficiencies were slightly lower than the inhalable curve for small particles at 1.0 and 1.5 m/s. Due to the effects of wind directions, the average data points showed a large bias. To compare the inhalable curve, the closest aspiration efficiencies were obtained at a wind speed of 0.5 m/s with an RMSD of 0.17. For the wind speeds of 1.0 and 1.5 m/s, the RMSDs to the inhalable curve are 0.34 and 0.31 respectively.

For the NIOSH sampler, the orientation-averaged data points were close to the inhalable curve at the three wind speeds. Most of the data were higher than the inhalable curve, especially the ones at the wind speed of 1.5 m/s. The RMSDs at these three wind speeds are very close (0.21, 0.27, and 0.29). The closest one was also at a wind speed of 0.5 m/s.

The aspiration efficiency for both types of samplers was highly affected by wind direction. The only one that had an RMSD below 0.2 was the PENS at a wind speed of 0.5 m/s when the sampling inlet was faced to the wind. The RMSD appeared larger than 0.3 for all other conditions. Only small particles (less than 2  $\mu\text{m}$ ) have the efficiency that close to the inhalable curve. Large particles had large deviations to the curve.

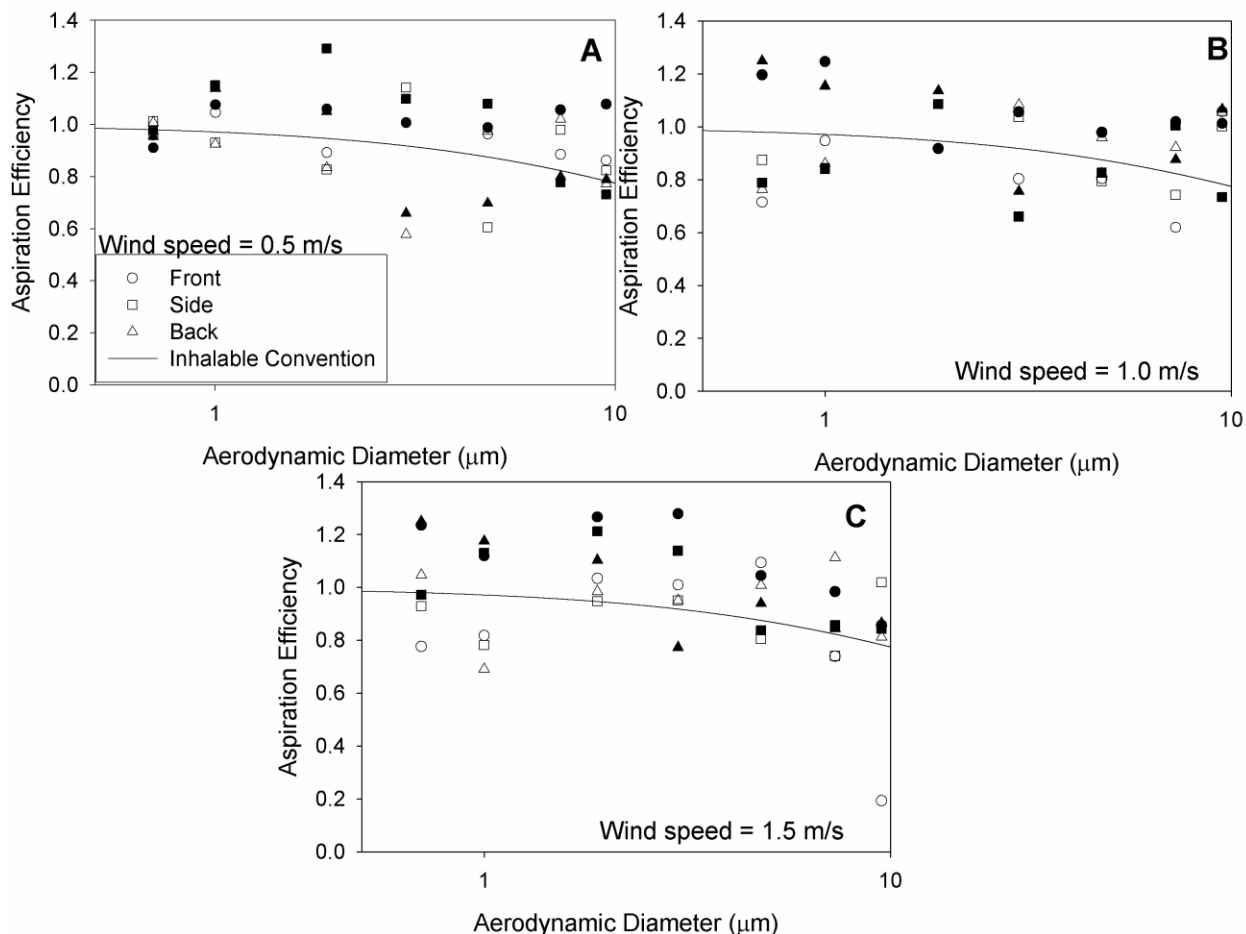


FIGURE 11. The aspiration efficiency as a function of particle size for different orientations at the wind speeds of 0.5 (A), 1.0 (B), and 1.5 (C) m/s. Empty symbols = PENS; blocked symbols = NIOSH.

In order to compare with other studies reported in pertinent literature, the aspiration efficiency was described as a function of Stokes number ( $Stk$ ), a dimensionless parameter, defined as  $d_{ae}^2 \rho_p U / 18 \mu \delta$ , where  $d_{ae}$  is the particle aerodynamic diameter,  $\rho_p$  is the density, and  $\mu$  is the viscosity of air, and  $\delta$  is the inner diameter of the sampler inlet. Figure 12 shows a comparison of aspiration efficiencies for the two test samplers and the IOM personal samplers for a large range of the wind speed (0.4-2.2 m/s) and velocity ratios ( $U/U_0 = 0.1 - 10.5$ ).

Velocity ratio ( $U/U_0$ ) is another factor that can affect the aspiration efficiency. The samplers tested in this study were designed with a much smaller inlet size than the regular personal samplers. This design results in a small velocity ratio. The range of the velocity ratio was from 0.1-0.7, which is much smaller in comparison to the IOM test (2.7) in a previous study. However, as seen in Figure 8, there are no significant differences between the studies. This indicates the velocity ratio may not be an issue within a certain particle size and wind speed.

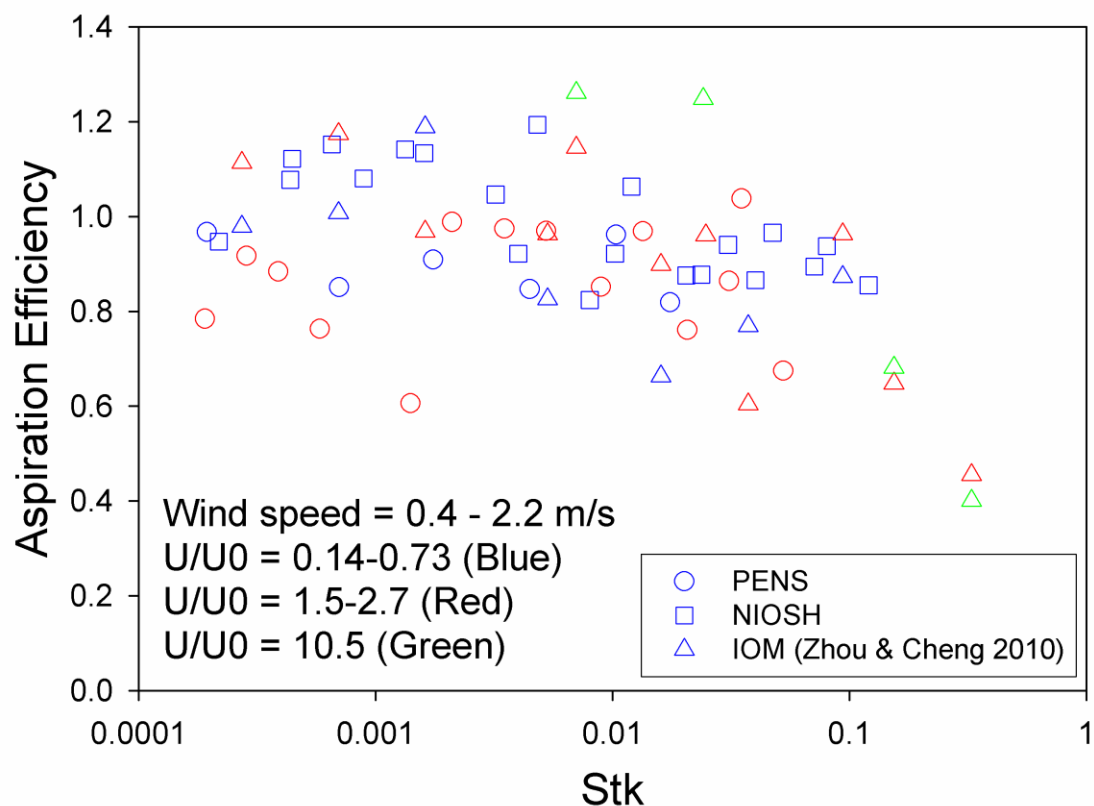


FIGURE 12. Personal sampler aspiration efficiency compared with reported data as a function of Stokes number at all wind speeds (0.4-2.2 m/s).

### 3. Specific Aim 3: To evaluate the performance of the sampler in collecting the nanoparticle fraction of nanomaterials

#### 3.1 Methodology

The performance of the personal nanoparticle sampler in the collection of engineered nanoparticles was evaluated by comparing the collection characteristics with the MOUDI impactor, which aerodynamically separates particles down to nanoparticle size fractions and collect these fractions on stages. The 3rd, 9th, and 10th stages of the MOUDI impactor were used in the experiment. The 50% cutpoint diameter of the 3rd stage was 3.2  $\mu\text{m}$ , which is similar to the cyclone stage of the PENS. The results from 9th stage, which has a cutpoint diameter of 92 nm, was compared with the impactor stage of the PENS (cutpoint = 95-100 nm). The result of last stage (10th) was compared with the backup filter of the PENS. A Teflon filter (PTU 1002550, Sterlitech Corp., Kent, WA) coated with silicone oil was used as the impaction substrate supported by the aluminum foil to avoid solid particle bounce. A 37-mm Cellulose filter (TE-241-37, Tisch Environmental, Cleves, OH) was used as backup filter.

### 3.1.1 Test nanomaterials and Nanoparticle generation methods

Titanium Dioxide ( $\text{TiO}_2$ , anatase, purity >99%; 10-25 nm, US Research Nanomaterials Inc., Houston, TX ) and Stacked-Cup Carbon Nanotubes (SCCNTs, >97%, Diameter=10-30nm, Length>2 $\mu\text{m}$ , Shenzhen Nanotech Port Co. Ltd, Shenzhen, China) were used as test material. A dry powder dispersion method developed by the NIOSH (Ku et al., 2006) was used to generate the CNT using a vortex shaker (Vortex Genie 2, Model G560, Scientific Industries Inc., Bohemia, NY) as shown in Figure 13.

### 3.1.2 Experimental Set-up

Figure 13 showed the experimental setup. Nanoparticles generated from the Vortex shaker passed through a impactor stage to remove larger particles. The test particles were then discharged and diluted with clean air in a mixing chamber. The sampling port was located at the other end of the chamber. After sampling, the substrates and filters were weighed by a balance (Sartorius CPS225D, Data Weighing Systems Inc., Elk Grove, IL).

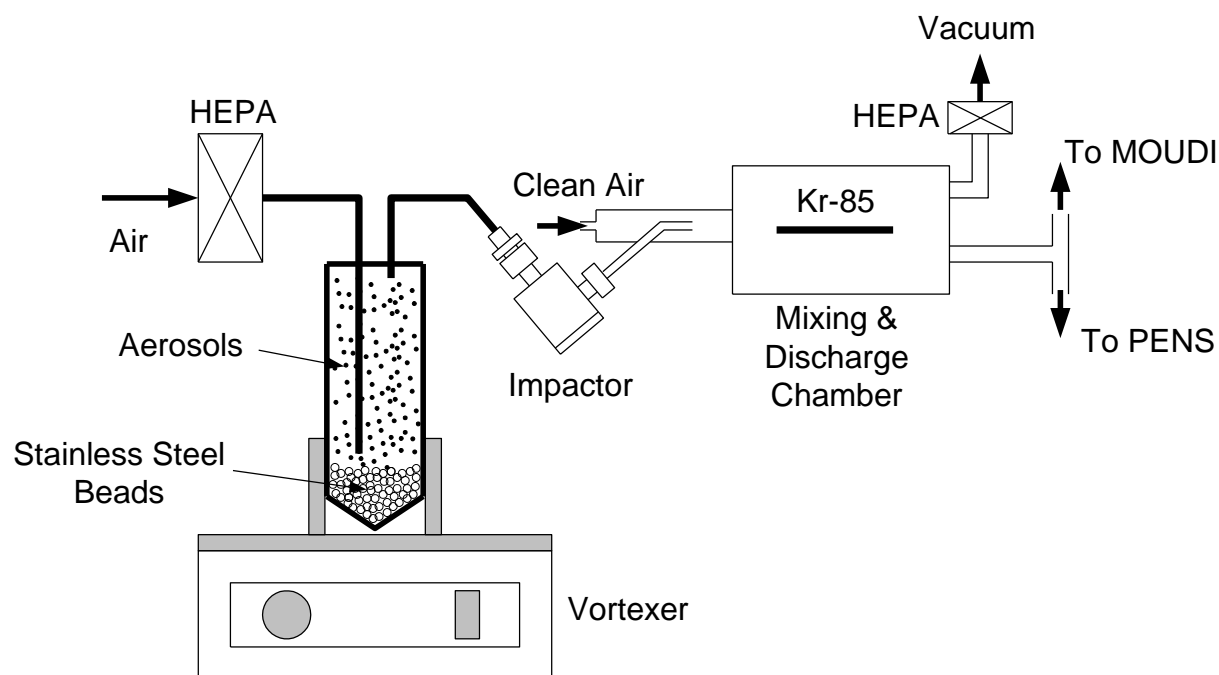


Figure 13. Experimental setup to compare the collection of nanomaterials in PENS and MOUDI.

## 3.2 Results

Figures 14 and 15 show the particle size distributions of  $\text{TiO}_2$  and CNT nanoparticles measured by using a 10-stage MOUDI impactor showing wide size distributions covering from 50 nm to 20  $\mu\text{m}$  similar to reported nanoparticle size distribution in the workplace. The mass median aerodynamic diameters of these two materials were 1.37 and 3.33  $\mu\text{m}$ , respectively for  $\text{TiO}_2$  and CNT. The geometric standard deviations were 2.77 and 3.53 for  $\text{TiO}_2$  and CNT, respectively.



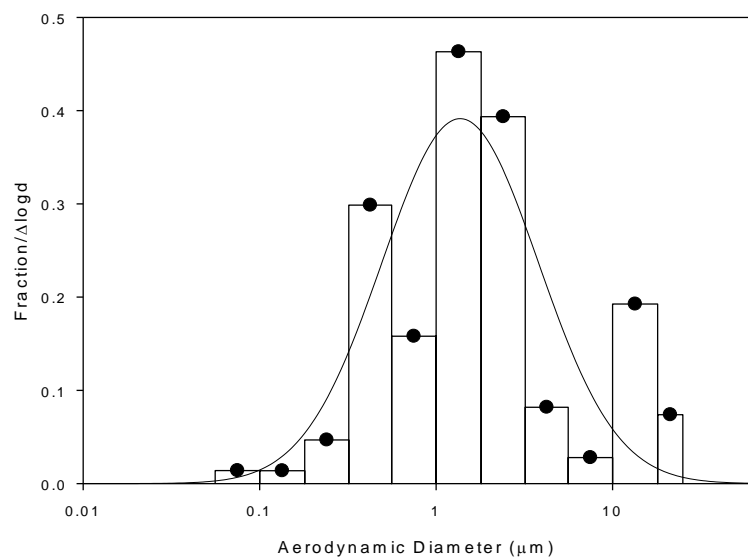


Figure 14. Particle size distribution of  $\text{TiO}_2$ .

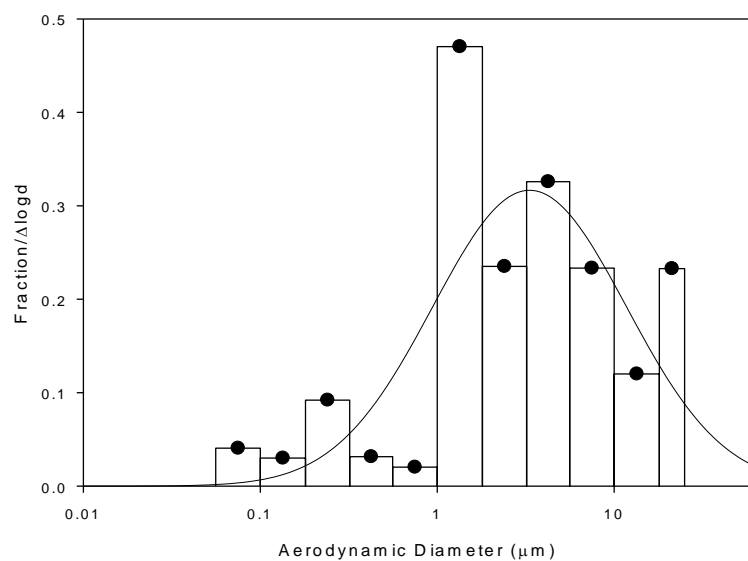


Figure 15. Particle size distribution of CNT.

Figure 16 shows comparison of particle concentration on samples collected on the PENS impactor stage with MOUDI stage #9 for  $\text{TiO}_2$  particles which would collect particles in the size range of 100 nm

to 4  $\mu\text{m}$  for the PENS and 100 nm to 3.2  $\mu\text{m}$ . Figure 17 shows comparison of particle concentration on samples collected on the PENS backup filter of PENS with MOUDI stage 10, which would collect particles in the size range smaller than 100 nm. The results show good agreement between the PENS and MOUDI stages for  $\text{TiO}_2$  particles.

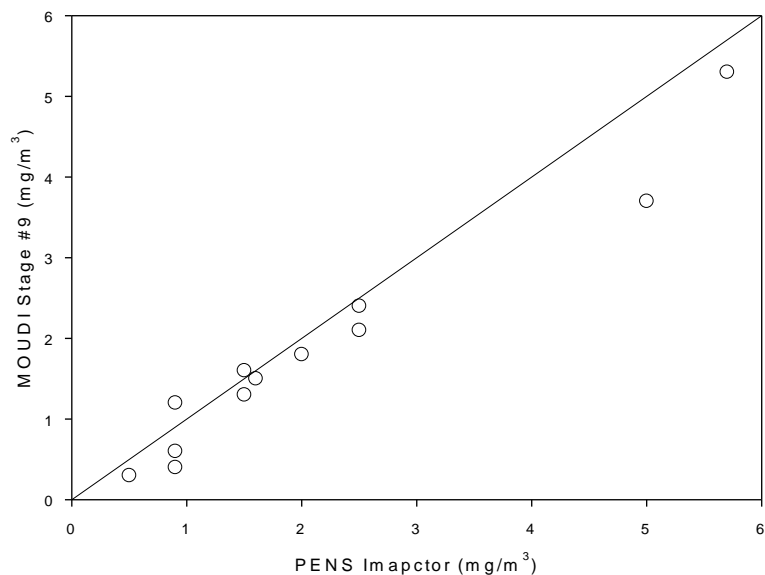


Figure 16. PENS impactor stage compared with MOUDI stage #9 for  $\text{TiO}_2$  particles.

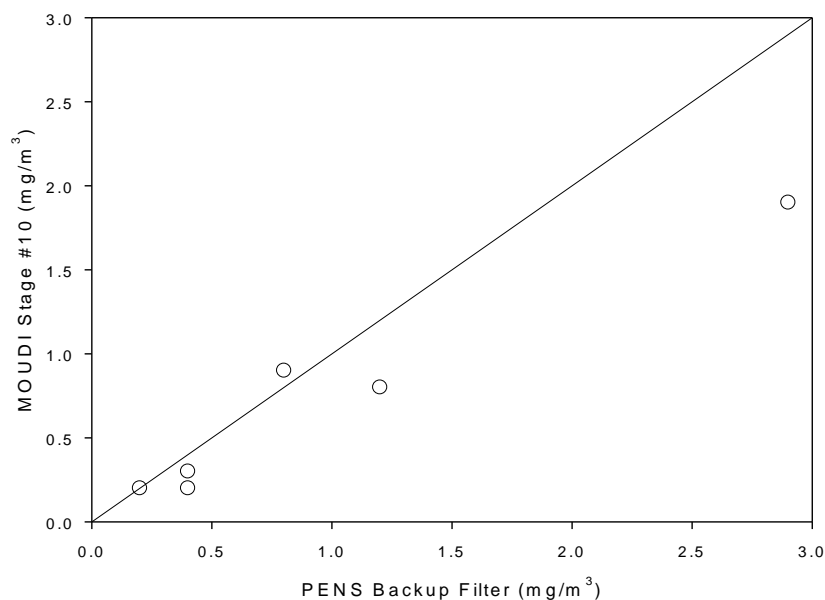


Figure 5. PENS backup filter compared with MOUDI stage #10 for  $\text{TiO}_2$  particles.

Figure 18 shows comparison of particle concentration on samples collected on the PENS impactor stage with MOUDI stage #9 for CNT particles which would collect particles in the size range of 100 nm to 4  $\mu\text{m}$  for the PENS and 100 nm to 3.2  $\mu\text{m}$ . Figure 19 shows comparison of particle concentration on samples collected on the PENS backup filter of PENS with MOUDI stage 10, which would collect particles in the size range smaller than 100 nm. The results show good agreement between the PENS and MOUDI stages for CNT particles.

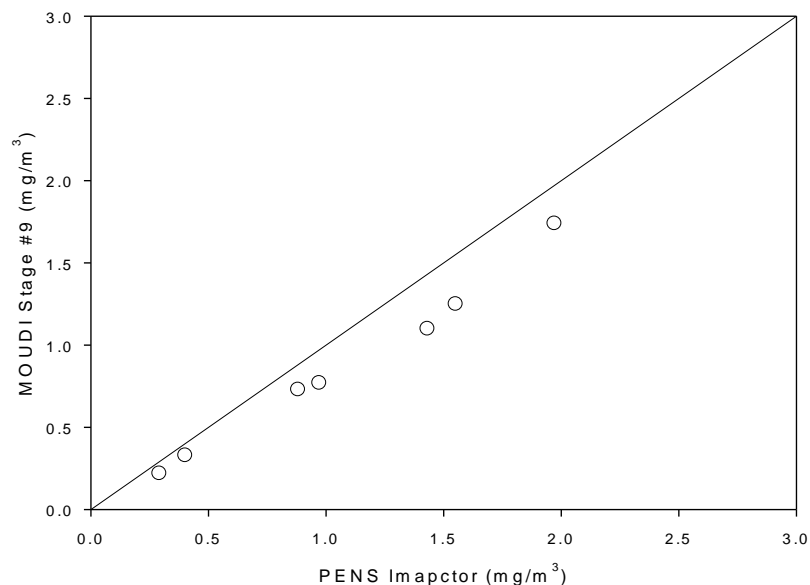


Figure 18. PENS impactor stage compared with MOUDI stage #9 for CNT particles.

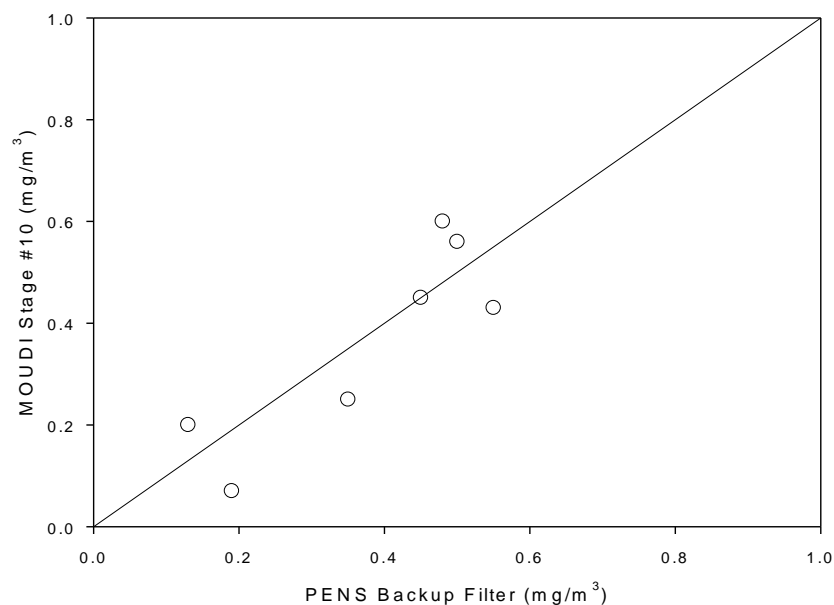


Figure 19. PENS backup filter compared with MOUDI stage #10 for CNT particles.

## 4. CONCLUSIONS

We developed a personal sampler capable of collecting the ultrafine particles (nanoparticles) in the occupational environment. This sampler consists of a cyclone for respirable particle classification, a micro-orifice impactor with a cutoff diameter of 100 nm for nanoparticle classification and a backup filter to collect nanoparticles.

Collection efficiencies of the cyclone and impactor stages were determined using monodisperse polystyrene latex and silver particles, respectively. Calibration of the cyclone and impactor stages showed 50% cut-off diameters of 4  $\mu\text{m}$  and 100 nm meeting the design requirements. Aspiration efficiencies of the sampler were measured in a wind tunnel at a flow rate of 2 L/min with wind speeds of 0.5, 1.0, and 1.5 m/s. The test samplers were mounted on a full size mannequin with three orientations toward the wind direction (0°, 90°, and 180°). Monodisperse oleic acid aerosols tagged with sodium fluorescein in the size range of 2 to 10  $\mu\text{m}$  were used in the test. For particles smaller than 2  $\mu\text{m}$ , the fluorescent polystyrene latex particles were generated by nebulizers. Results showed that the orientation-averaged aspiration efficiency for both samplers were close to the inhalable fraction curve. Our evaluation showed that the current design of the personal sampler met the designed criteria for collecting nanoparticles  $\leq 100$  nm in occupational environments.

Comparison of  $\text{TiO}_2$  and carbon nanotube nanoparticles collection in the personal sampler with MOUDI impactor show good agreement indicating that the personal sampler is useful for collecting nanoparticles.

## PUBLICATIONS

### Publications Generated from the Present NIOSH-funded Study

1. Su WC, Tolchinsky AD, Sigaev VI, Cheng YS: [2011] Performance Evaluation of Two Personal Bioaerosol Samplers. *Journal of Environmental Science and Health, Part A* 46 1690-1698.
2. Tsai CJ, Liu CN, Huang SM, Chen SC, Huang SN, Cheng YS, Zhou Y: [2012] A Novel Active Personal Nanoparticle Sampler (PENS) for the Exposure Assessment of Nanoparticles in Workplaces. *Environmental Science and Technology* 46(8):4546-4552.
3. Su WC, Tolchinsky AD, Sigaev VI, Cheng YS: [2012] A Wind Tunnel Test of Newly Developed Personal Bioaerosol Samplers, *Journal of the Air & Waste Management Association* 62(7): 828-837.
4. Cheng, YS, Su, W: [2013] Thoracic Fraction of Inhaled Fiber Aerosol. *Journal Occupational Environmental Hygiene* 10(4): 194-202.
5. Zhou, Y, Irshad, H, Tsai, CJ, Huang, SM, Cheng, YS: [2014] Evaluation of a Novel Personal Nanoparticle Sampler. *Environmental Science Processes Impacts* 16:203-210.
6. Cheng, YS: [2014] Pharmaceutical Aerosol Deposition in the Respiratory Tract. *AAPS Pharmaceutical Science Technology* 15(3): 630-640.
7. Cheng, YS, Zhou, Y, and Su, WC: [2014] Deposition of Particles in Human Mouth-Throat Replicas and a USP Induction Port. *J. Aerosol Medicine Pulmonary Drug Delivery*, doi:10.1089/jamp.2013.1105.

8. Cheng, YS, and Su, WC: Characterization of Carbon Nanotube Particles: Morphology and Equivalent Diameters. *Aerosol Sci. Technol.* (submitted).

## REFERENCES

- Asgharian, B. and Price, OT: [2007] Deposition of ultrafine (nano) particles in the human lung. *Inhal. Toxicol.* 19:1045-1054.
- Azong-Wara, N, Asbach, C, Stahlmecke, B, Fissan, H, Kaminski, H, Sabine, P, Kuhlbusch, TAJ.: [2009] Optimisation of a thermophoretic personal sampler for nanoparticle exposure studies. *J. Nanopart. Res.* 11(7):1611-1624.
- Biswas, P, and Wu, CY: [2005] Nanoparticles and the environment - A critical review paper. *J. Air Waste Manage. Assoc.* 55:708-746.
- Blachman, MW, and Lippmann, M: [1974] Performance characteristics of the multicyclone aerosol sampler. *Am. Ind. Hyg. Assoc. J.* 35:311-326.
- Cheng, YS, Smith, SM, Yeh, HC, D.B. Kim, K.H. Cheng, and D.L. Swift: Deposition of ultrafine aerosols and thoron progeny in replicas of nasal airways of young children. *Aerosol Sci. Tech.* 23:541-552 (1995).
- Cheng, YS, Yeh, HC, Guilmette, RA, Simpson SQ, Cheng, KH, and Swift, DL: [1996] Nasal deposition of ultrafine particles in human volunteers and its relationship to airway geometry. *Aerosol Sci. Technol.* 25:274-291.
- Cheng, YS, Irshad, H, McFarland, AR, Su, WC, Zhou, Y, and Barringer, D: [2004] An aerosol wind tunnel for evaluation of massive-flow air samplers and calibration of snow white sampler. *Aerosol Sci. Technol.* 38:1099-1107 (2004).
- Cohen, BS and Asgharian, B: [1990] Deposition of ultrafine particles in the upper airways: an empirical analysis. *J. Aerosol Sci.* 21:789-797.
- Demou, E, Peter, P, and Hellweg, S: [2008] Exposure to manufactured nanostructured particles in an industrial pilot plant. *Ann. Occup. Hyg.*, 52:695-706.
- Fissan, H, Neumann, S, Trampe, A, Pui, DYH, and Shin. WG: [2007] Rationale and principle of an instrument measuring lung deposition nanoparticle surface area. *J. Nanoparticle Res.*, 9:53-59.
- Hoet, PHM, Ruske-Hohlfeld, I, and Salata, OV: [2004] Nanoparticles—known and unknown health risks. *J. Nanobiotechnol* 2:12-26.
- Kreyling, W, Semmler, M, and Moller, W: [2004] Dosimetry and toxicology of ultrafine particles. *J. Aerosol Med.* 17:140-152.
- Lindsley, WG, Schmechel, D, and Chen, BT: [2006] A two-stage cyclone using microcentrifuge tubes for personal bioaerosol sampling. *J. Environ. Monit.* 8:1136–1142.
- Lorenzo, R, Kaegi, R, Gehrig, R, Scherrer, L, Grobety, B, Burtcher, H: [2007] A thermophoretic precipitator for the representative collection of atmospheric ultrafine particles for microscopic analysis. *Aerosol Sci. Technol.* 41(10): 934-943.
- Marple, VA, Rubow, KL, Behm, SM: [1991] A microorifice uniform deposit impactor (MOUDI): Description, calibration and use. *Aerosol Sci. Technol.* 14(4):434-446.
- Maynard, AD, Baron, PA, Foley, M, Shvedova, AA, Kisin, ER, and Casuccio, GS: [2004] Exposure to carbon nanotube material: aerosol release during the handling of unrefined single-walled carbon nanotube material. *J. Toxicol. Environ. Health* 67A:87-107.

- Miller, A, Frey, G, King, G, Sunderman, CA: [2010] Handheld electrostatic precipitator for sampling airborne particles and nanoparticles. *Aerosol Sci. Technol.* 44(6):417-427.
- Oberdorster, G, Oberdorster, E, and Oberdorster, J: [2005] Nanotoxicity: an emerging discipline evolving from studies of ultrafine particles. *Environ. Health Perspect.* 113:823-839.
- Phalen, RF, Hinds, WC, John, W, Liou, PJ, Lippmann, M, McCawley, MA, et al. [1986]: Rationale and recommendations for particle size-selective sampling in the workplace. *Appl Ind Hyg* 1:3-12.
- Rubow, KL, Marple, VA, Olin, JG, McCawley, MA: [1987] A personal cascade impactor: design, evaluation and calibration. *Amer. Ind. Hyg. Assoc. J.* 48 (6):532-538.
- Smith, SM, Cheng, YS and Yeh, HC: [2001] Deposition of ultrafine particles in human tracheobronchial airways of adults and children. *Aerosol Sci. Technol.*,35:697-709-709.
- Thayer, D, Koehler, KA, Marchese, A, Volckens, J: [2011] A personal thermophoretic sampler for airborne nanoparticles. *Aerosol Sci. Technol.* 45(6):744-750.
- Tsai, CJ, Shiau, HG, Shih, TS: [1999] Field study of the accuracy of two respirable sampling cyclones. *Aerosol Sci. Technol.* 31(6):463-472.
- Wang, SC, and Flagan, RC: [1990] Scanning electrical mobility spectrometer. *Aerosol Sci. Technol.* 13:230-240.
- Yeganeh, B, Kull, CM, Hull, MS, and Marr, LC: [2008] Characterization of airborne particles during production of carbonaceous nanomaterials. *Environ. Sci. Technol.* 42:4600-4606.
- Zhou, Y and Cheng, YS: [2010] Evaluation of IOM personal sampler at different flow rates. *J. Occup. Environ. Hyg.* 7:88-93.